D6.5: Demonstration of water resources management services for the Brahmaputra basin

Project number
313238

Project title
LOTUS— Preparing Land and Ocean Take Up from Sentinel-3

Call (part) identifier
FP7-SPACE-2012-1

Funding scheme
Collaborative project

Deliverable Number D6.5
Title: “Demonstration of water resources management service for the Brahmaputra basin.”

Nature: Report

Dissemination level: Public

Status: v1.0

Date: 2015-12-22

Author list

Author	Affiliation
Peter Bauer-Gottwein	DTU Environment, Denmark
Raphael Schneider	DTU Environment, Denmark
Henrik Madsen	DHI, Denmark
Marc Ridler	DHI, Denmark
Peter Nygaard	DHI, Denmark

DOCUMENT CHANGE LOG				
Rev.	Date	Sections modified	Comments	Changed by
1	22 Dec 2015	All		All authors

Acronyms

CRPS	Continuous ranked probability score
DEM	Digital elevation model
EKF	Extended Kalman filter
EnKF	Ensemble Kalman filter
ETKF	Ensemble transform Kalman filter
MAE	Mean absolute error
ME	Mean error (bias)
NAM	Nedør-Afstrømnings model (Danish for rainfall-runoff model)
NSE	Nash-Sutcliffe model efficiency
PDF	Probability density function
Rating curve	Empirical relationship between river water level and river discharge
RMSE	Root mean square error
SAR	Synthetic aperture radar
SWOT	Surface Water and Ocean Topography mission
Virtual station	Crossing between the satellite ground track and a river

1 Table of Contents

2 Executive summary

This report has been prepared as part of the project 'Preparing Land and Ocean Take Up from Sentinel-3 (LOTUS)' Work Package 6 'Applications of new GMES data in value-adding land services', Deliverable 6.5.

The report presents a proof-of-concept for how to use CryoSat drifting orbit radar altimetry data together with hydrologic-hydrodynamic models. The generic workflow described in LOTUS D6.4 is applied to the Brahmaputra river system in South Asia. CryoSat data is used twice in this workflow:

1. To update the river bed elevation and cross sectional geometry of the hydrodynamic model
2. To update simulated water level states in the hydrodynamic model online, using data assimilation techniques.

Results show that water surface elevation estimates from CryoSat contain useful information and improve the sharpness and reliability of hydrologic predictions in this basin.

3 Introduction

Space-borne measurements of inland water surface elevation from radar and laser altimetry have been provided by a number of remote sensing missions over the past ca. 20 years. Because the sampling pattern of these missions is sparse and irregular in space and time, such data has to be combined with hydrologic-hydrodynamic simulation models in order to fully exploit the information contained in the data. Data assimilation is a generic approach to combine observational data and simulation models, which is widely used in all branches of earth science, including atmospheric science, oceanography and hydrology. Assimilation of repeat-orbit radar altimetry has been successfully demonstrated before; however, LOTUS is one of the first projects to attempt assimilation of drifting-orbit (CryoSat-type) altimetry data to hydrologic-hydrodynamic models. The principal challenge is that this type of mission provides individual water height readings somewhere on the river, which cannot be collected into a time series at a so-called virtual station (VS), as was the case with previous missions.

A number of recent studies combine satellite radar altimetry with hydrologic river models using data from repeat orbit satellites such as Envisat, ERS or Jason. One popular river is the Amazon due to its large size and favourable direction of flow in relation to most satellites' orbits, for example Yamazaki et al. (2012). Other examples include other big rivers, such as the Mekong and Ob in the work of Birkinshaw et al. (2014) where daily discharge data was estimated from Envisat and ERS-2 altimetry. A combination of MODIS data of river velocity and Envisat water levels was used by Tarpanelli et al. (2014) to estimate the discharge in the Po River. Using satellite altimetry data is particularly attractive over poorly gauged basins where in-situ data is lacking. Becker et al. (2014) have used Envisat altimetry data in the Congo basin. Moreover, application of data from the wide-swath drifting orbit mission SWOT has been considered (for example Biancamaria et al. (2011a) or Yoon et al. (2012)), however only with synthetically generated data: The SWOT mission is expected to be launched in 2020 NASA, 2015.

The CyoSat-2 data used in this work have already been shown by Villadsen et al. (2015) to be useful to monitor water levels in the Ganges and Brahmaputra. There also exist a number of studies using CryoSat-2

altimetry to extract water levels in lakes, for example Kleinherenbrink et al. (2014) or Song et al. (2015). This work however is one of the first applications of CryoSat-2 altimetry over rivers, showing how its special drifting orbit can be used.

In a previous study at DTU Environment, Michailovsky et al., 2013 assimilated Envisat altimetry data at multiple VS into a routing model of the Brahmaputra using an extended Kalman filter (EKF) approach. The present study extends this work to enable the assimilation of Cryosat data. The main modifications are

- The routing scheme is replaced with a 1-D hydrodynamic modeling scheme based on the full Saint-Venant equations for open channel flow (dynamic wave). This scheme simulates the true river water level anywhere along the river.
- Due to the strongly non-linear nature of the hydrodynamic model the EKF is replaced with an ensemble approach.
- The modeling system is implemented in the DHI hydrologic-hydrodynamic simulation environment. This environment also provides a generic data assimilation toolbox, which gives access to a number of different ensemble-based assimilation routines (please see LOTUS D6.4 for details)
- Parameterization of model and observation error are similar to Michailovsky et al., 2013.

4 Description of the Brahmaputra case study

For the Brahmaputra basin in South Asia, previous work has shown the value of Envisat altimetry data (Michailovsky et al., 2013). The basin and its main river, the Brahmaputra, are being monitored closely by India and China, however almost none of this in-situ hydrologic data is publicly available. The Brahmaputra catchment for example is considered a classified basin by the Indian government (Central Water Commission, 2009). This situation highlights the importance of remote sensing data for hydrologic modelling and water resources management in the basin, for instance for flood forecasting in downstream Bangladesh. Bangladesh, a low lying country facing the Gulf of Bengal in the estuary region of the three large rivers Ganges, Brahmaputra and Meghna (see Figure 1), is often hit by devastating floods. More than 90% of its surface waters are imported from beyond the country's boundaries, i.e. mainly India; however, mechanisms for sharing of data and information between Bangladesh and India are not in place (Biancamaria et al., 2011b).

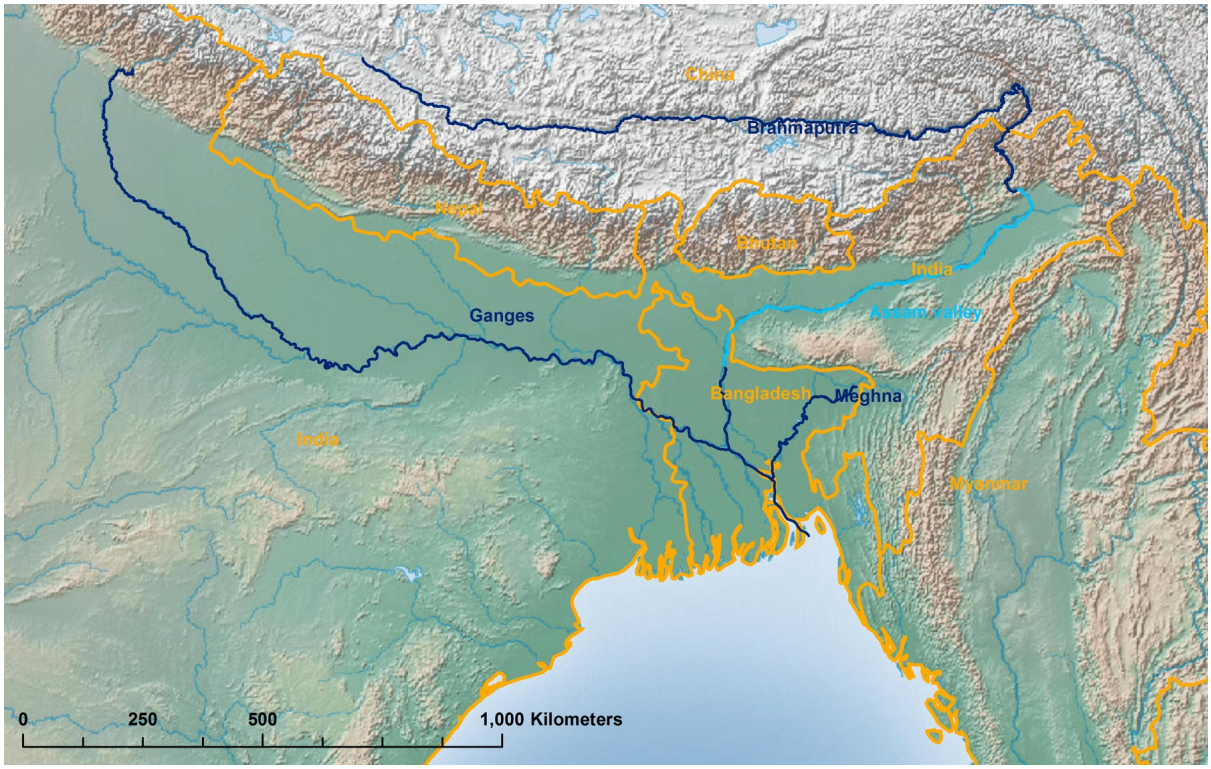

Figure 1: Map of the three main rivers draining into the Gulf of Bengal through Bangladesh. The stretch of the river that is referred to as "Assam Valley" in the text is colored in cyan.

4.1 Physiography of the region

The course of the Brahmaputra River can be roughly divided into two parts: The upstream part in the Tibetan Plateau draining through the Himalaya into India, and the downstream part, which drains through the Assam valley into Bangladesh where it merges into the Ganges-Brahmaputra-Meghna delta region and finally flows into the Gulf of Bengal. In the downstream part (elevation below 200 mamsl) river slopes are mild and the Brahmaputra is a wide braided river. In the upstream part however the river width usually is below 500 meters, and the river is often surrounded by steep slopes. The elevation is generally above 3000 mamsl and river slopes are variable; steep gorges alternate with milder slopes (Figure 5). This makes it hard to extract satellite altimetry data, and therefore the focus of this study was on the Assam valley part of the river. The climate in the region is dominated by the South-Asian monsoon, featuring a strong seasonality of precipitation with the rainy season in the period from late June to September. Precipitation is strongest on the south side of the Himalayan slopes, while the Tibetan portion of the river receives less precipitation. The hydrology of the high-elevation portions of the basin is dominated by snow accumulation and snow melt as well as glacial dynamics.

4.2 CryoSat-2 dataset for the Brahmaputra

We used CryoSat-2 level 2 altimetry data that was processed and provided by DTU Space in the framework of the LOTUS project. The basis for the data is the ESA baseline-b L1b 20 Hz product. This product was retracked by Villadsen et al. (2015) using a primary peak threshold retracker. Most of the study area is covered in the dense SARIn mode of CryoSat-2. The data is available since July 2010. For this report, data until the end of 2013 have been used.

4.3 Preprocessing of the data

The CryoSat-2 dataset currently does not deliver reliable information on whether individual waveforms were acquired over water (river) or over land surfaces. Sometimes, the backscatter values (sigma0) can give an indication of the type of surface an individual echo was acquired over. Over the Brahmaputra however, the backscatter values could not be used, which might be due to the fact that the river is relatively narrow and its waters often turbulent or turbid and consequently cannot be distinguished from land surfaces. Hence, the distinction between CryoSat-2 data points representing river water surface and land surface has to be based on independent data – in this case a water mask from multispectral satellite imagery. Moreover, the Brahmaputra in the Assam valley is a very dynamic braided river and experiences significant changes to its course from one year to another (see Figure 2), which requires dynamic river masks.

Figure 2: Landsat 7 image of the same part of the Brahmaputra river in the Assam valley showing the dynamic changes in river morphology. Left: 2010. Right: 2011.

4.3.1 Landsat river mask

For mapping the dynamic braided river system, high resolution multi-temporal data with at least a seasonal time step is needed. Because no SAR data covering the entire period of interest is freely available, it was decided to use optical imagery from the Landsat program.

Landsat 7 and 8 NDVI imagery is available every 8 days, however due to issues such as cloud cover and sensor failures only 32-day composites give a reasonable result (Google, 2015). All areas with an NDVI below 0 were considered water, everything else was considered land. Because of the above mentioned morphological dynamics, an individual mask had to be created for each year from 2010 to 2013. However, even using the 32-day composites no sufficient coverage could be achieved during the high-flow season in summer due to cloud cover. Thus, minimum water extent masks were created by merging all available images from one year. For a pixel to be classified as water in the minimum water extent mask, it had to be classified as water in each individual 32-day composite image of the year.

4.3.2 Filtering and projecting the CryoSat-2 data

Figure 3 shows the filtering and projection process applied to the CryoSat-2 level 2 data points. Only data points above the Landsat minimum river mask for the respective year are used, i.e. considered to represent the river water surface. After filtering, the points have to be projected on the river line of the 1D hydrodynamic model to determine the correspondence between CryoSat 2 observation location and model state space (Figure 3). Points were subsequently divided into separate groups based on their distance from each other using an automatic k-means clustering algorithm and heights averaged for each group separately (Figure 4). For technical details on this procedure, please refer to LOTUS D 6.4.

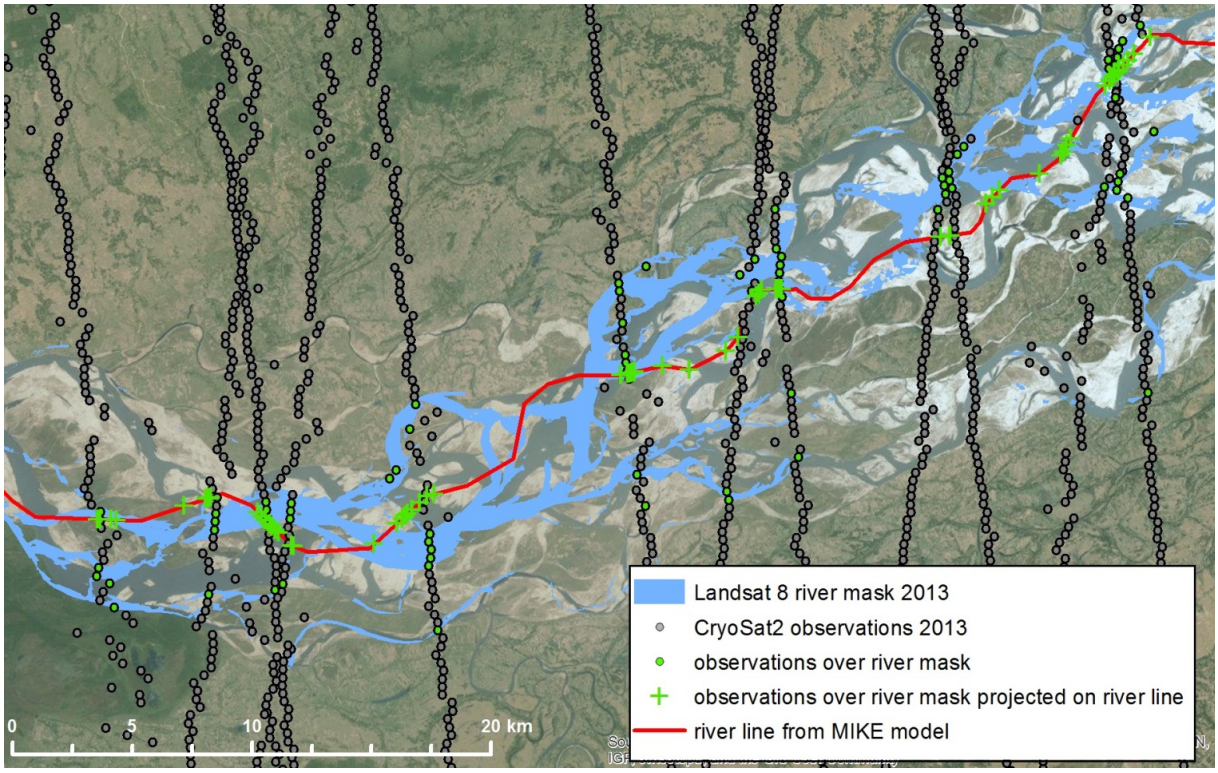

Figure 3: Section of the Brahmaputra in the Assam valley showing the Landsat river mask, the CryoSat-2 observations and their mapping to the 1D river model, all for 2013.

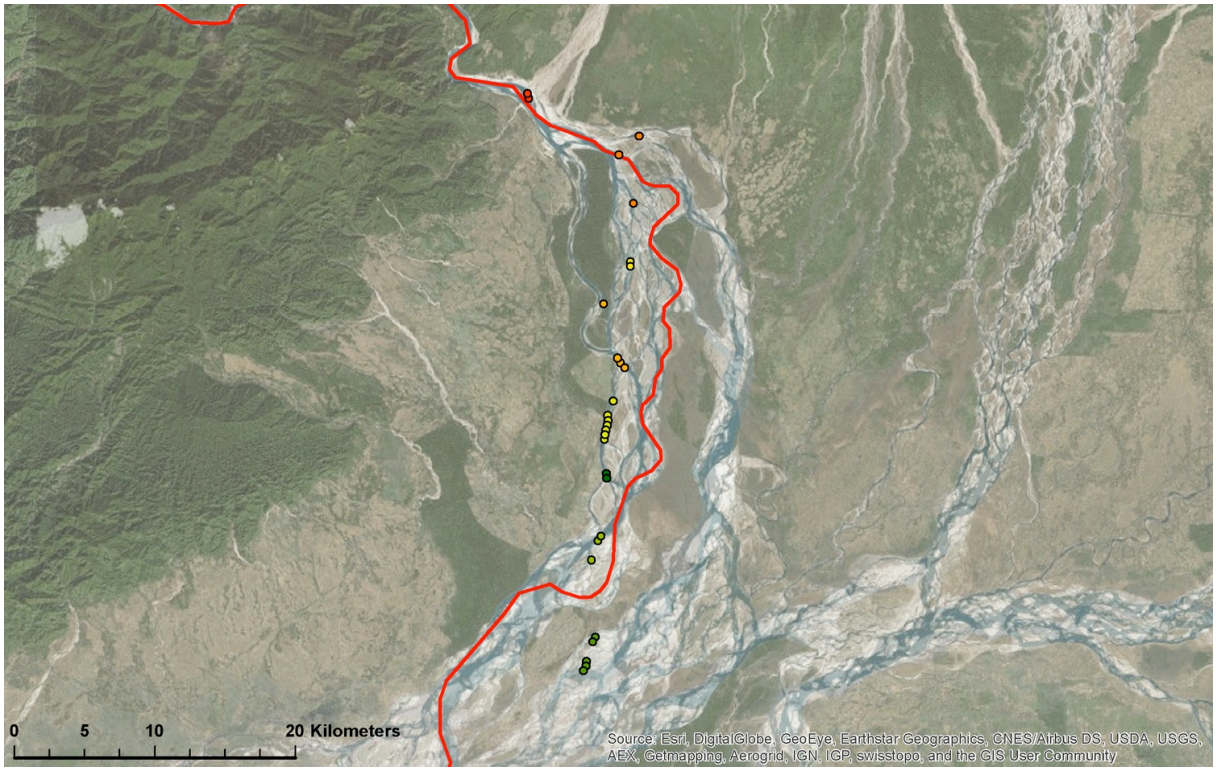

Figure 4: Spatial detail of one overflight showing the effect of the k-means clustering algorithm. All individual echoes are from the same overflight. All echoes shown in the same color are averaged into one single height estimate.

A summary of the available CryoSat altimetry data is shown in Table 1. Statistics for the headwater region and the Assam valley region are reported separately for each year of the record. We report both the number of individual returns over the water mask and the number of individual overflights of the water mask.

Table 1: Overview of available CryoSat-2 data over the Brahmaputra

	Assam Valley		Headwaters		Entire Brahmaputra	
	Number of returns over water	Number of overflights	Number of returns over water	Number of overflights	Number of returns over water	Number of overflights
2010	270	42	198	60	468	102
2011	1005	151	613	195	1618	346
2012	657	145	687	219	1344	364
2013	887	148	625	203	1512	351
Total	2819	486	2123	677	4942	1163

In order to minimize possible contamination of CryoSat data points by land returns, we investigated the effect of introducing a buffer zone around the edge of the water mask: Only points which are placed a minimum distance away from the edge of the water mask were considered true water echoes. Table 2 shows that, while the number of returns decreases strongly with the introduction of a buffer zone, the number of overflights remains more or less unchanged, at least for the Assam valley. Because all data points from the same overflight are acquired roughly at the same point in space and time, the data coverage does not decrease significantly with the introduction of a buffer zone.

Table 2: Number of CryoSat data points for different widths of the buffer zone

	Assam Valley		Headwaters		Entire Brahmaputra	
	Number of returns over water	Number of overflights	Number of returns over water	Number of overflights	Number of returns over water	Number of overflights
No buffer	2819	486	2123	677	4942	1163
30 m buffer	2444	467	1199	511	3643	978
60 m buffer	1989	458	595	295	2584	753

Figure 5 shows the CryoSat-2 data after filtering over the Brahmaputra river mask and projecting it onto the model's river line. The CryoSat-2 data shows many outliers, mainly in the upstream (Tibetan) part before river km 2000. In this area, the river is narrow and the terrain surrounding the river is very steep, explaining some of the outliers. In this portion, the results are very sensitive to the roll bias correction applied to the CryoSat-2 data. Still, meaningful data can be gathered in many places, as can be seen when compared to SRTM elevations along the same river line. If outliers in the CryoSat-2 data are defined as showing an elevation difference of more than 20 meters from the SRTM data, about 20% of the data are classified as outliers.

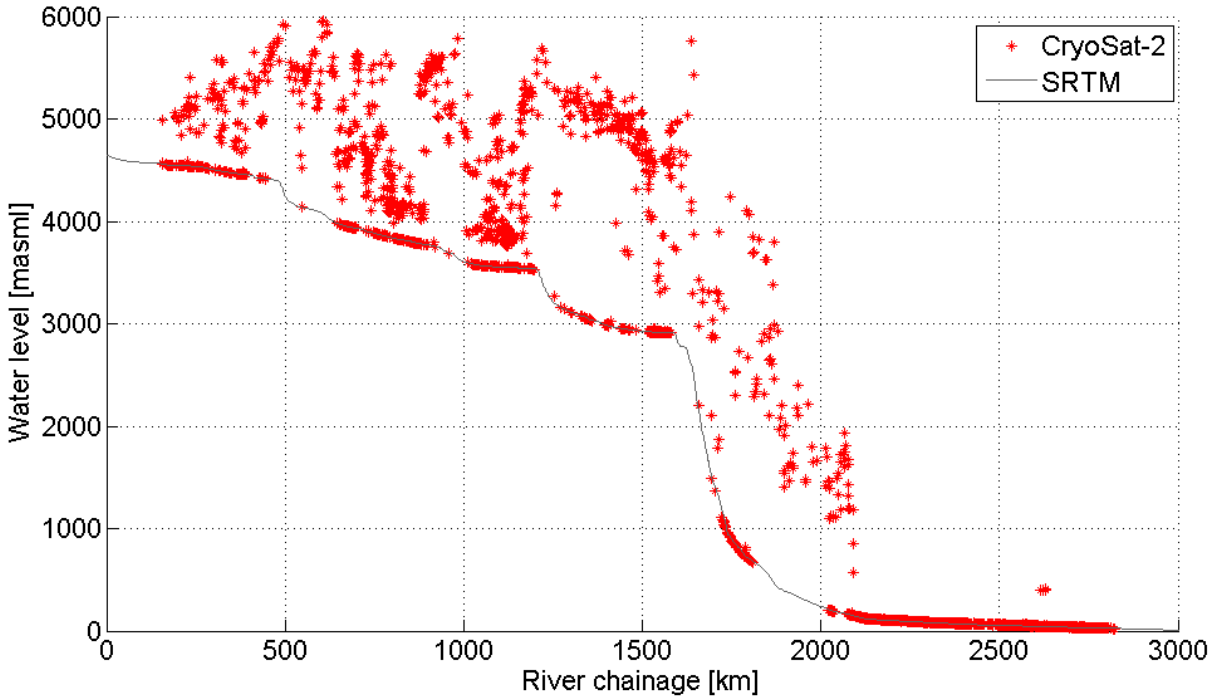

Figure 5: CryoSat-2 data 2010 to 2013 after filtering and mapping to the model's river line in comparison with SRTM data

5 Hydrologic-hydrodynamic modeling for the Brahmaputra

5.1 Rainfall-runoff model

Initially, a hydrologic-hydrodynamic model for the entire Ganges and Brahmaputra basin was set up in the DHI MIKE 11 software (Figure 6). The model consists of a hydrologic and a hydrodynamic part. The rainfall-runoff response is simulated using the NAM (Nedbør-Afstrømnings Model, Danish for rainfall-runoff model, Nielsen and Hansen, 1973). The runoff is generated in 87 lumped NAM rainfall-runoff subcatchments – 33 in the Brahmaputra basin and 54 in the Ganges basin. The runoff from individual catchments is added to the river network and discharge is routed through the river network in MIKE 11 using a 1D dynamic wave routing based on the Saint Venant equations for unsteady flow. For details on the hydrologic-hydrodynamic modeling approach, please refer to LOTUS D6.4.

For some of the NAM subcatchments, mainly in the Nepalese regions of the Ganges basin, in-situ discharge observations were available. Furthermore, discharge observations from the stations Bahadurabad on the Brahmaputra, and Hardinge Bridge on the Ganges (see Figure 6), both close to the two rivers' confluence, were available. Besides these few in-situ observations the entire model was based on remote sensing data: For the precipitation forcing, TRMM v7 3B42 data was used (Tropical Rainfall Measurement Mission Project (TRMM), 2011). Temperature and reference evapotranspiration was based on data from the APHRODITE's Water Resources project (APHRODITE's Water Resources, 2014). The SRTM DEM (Jarvis et al., 2008) was used to delineate the subcatchments and the drainage network. The calibration period included the years 2002 to 2007.

The rainfall-runoff models in the NAM subcatchments with available discharge observations were calibrated individually, and the resulting parameters transferred to the remaining catchments. As it was

impossible to generate enough runoff from the model especially in the Himalaya it was assumed that there is a bias in the TRMM precipitation data: For all Himalaya subcatchments the precipitation forcing was scaled with a factor of 1.1. Such a bias in the TRMM precipiation product has been found before, for example by Michailovsky et al. (2013).

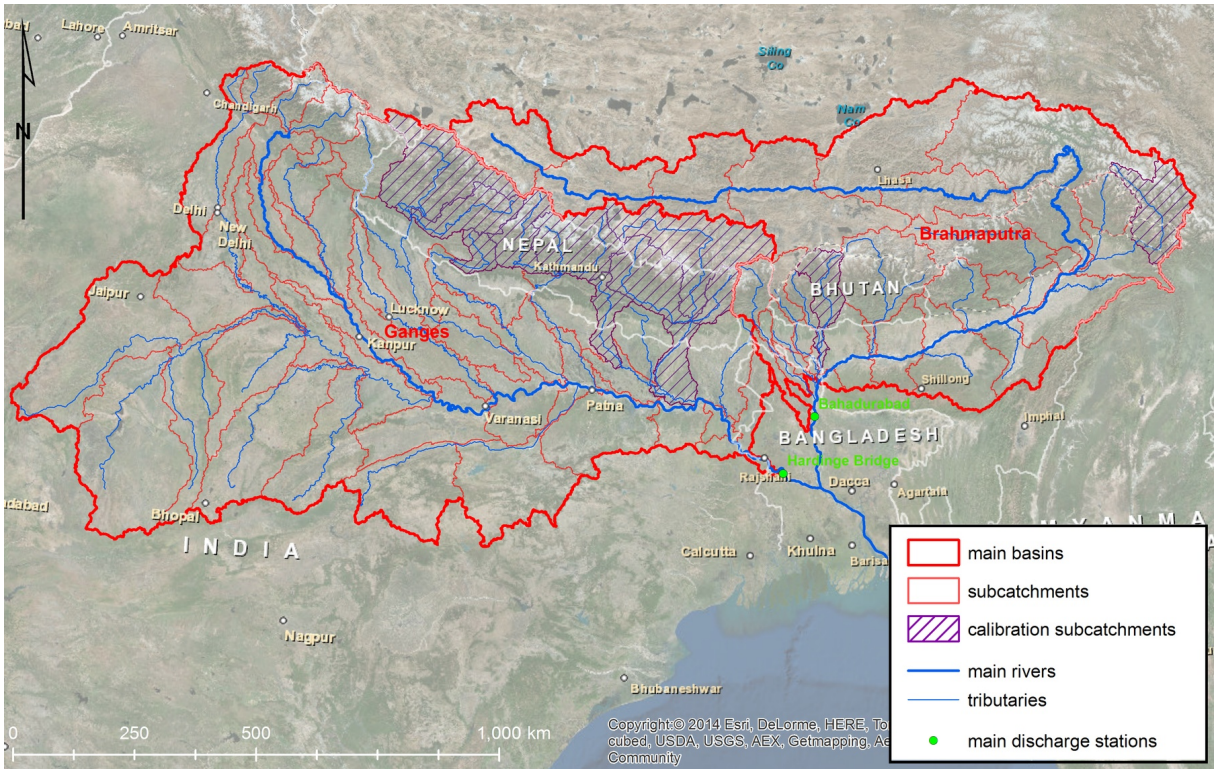

Figure 6: The Ganges-Brahmaputra basin model. Main basins as well as subcatchments are shown. Calibration subcatchments (Table 3) are hatched.

Table 3 provides an overview of rainfall-runoff model performance in the calibration catchments. With a few exceptions, performance statistics such as Nash-Sutcliffe model efficiency (NSE), root mean square error (RMSE) and mean error (bias, ME) are acceptable. Table 4 shows selected hydrologic indicators for all simulated subcatchments in the Brahmaputra. Runoff coefficients in all catchments are generally high and exceed 1 for the high-elevation catchments in the Brahmaputra, indicating long-term snow and ice loss in those catchments.

Table 3: Performance indicators for the calibration catchments

Calibration catchment	NSE (-)	RMSE (m^3/s)	ME (m^3/s)	Mean of observations (m^3/s)	Number of simulated observations
Arun	-0.7083	571	241	529	2189
Bagmati	0.1246	314	118	110	2190
Bheri	0.8182	144	34	307	2190
Gandhak 1	0.7880	557	67	955	2190

Kaligandaki	0.6898	263	10	403	2128
Karnali	0.6961	274	-101	513	2190
Lohit	0.0974	1007	234	919	2190
Rapti 1	0.5277	155	-15	115	1461
Sankosh 1	0.6577	186	32	348	2190
Sunkoshi	-0.6730	1102	-688	745	2190
Tamor	0.7465	252	-25	416	2190

Table 4: Selected hydrologic indicators for the simulated rainfall-runoff response in the NAM catchments

Catchment	Mean precipi-tation ($mmyr^{-1}$)	Mean runoff ($mmyr^{-1}$)	Median runoff ($mmyr^{-1}$)	Runoff 90-percentile ($mmyr^{-1}$)	Runoff-coeffi-cient (-)	Average snow storage (mm)	Average elevation (mamsl)
BMAPUTRA1	339	132	39	292	0.389	46.3	5109
BMAPUTRA2	270	219	57	455	0.811	37.7	5107
BMAPUTRA3	141	230	53	570	1.631	26.3	5029
BMAPUTRA4	235	232	116	1056	0.987	26.5	4839
BMAPUTRA5	195	252	122	1059	1.292	17.5	4837
BMAPUTRA6	281	419	123	757	1.491	15.0	4574
BMAPUTRA7A	553	664	651	3054	1.201	25.6	4396
BMAPUTRA7B	7145	5430	2142	5249	0.760	0.5	1802
BMAPUTRA8	4106	2015	581	1611	0.491	0.0	891
BMAPUTRA9	3541	1759	773	2843	0.497	0.0	430
BMAPUTRA10	2247	1146	588	2357	0.510	0.0	995
BMAPUTRA11	2732	1500	758	3212	0.549	0.0	487
BMAPUTRA12	3611	2222	559	2401	0.615	0.0	422
BMAPUTRA14	4288	2295	496	2250	0.535	0.0	273
BMAPUTRA15	4277	2134	60	230	0.499	0.0	116
SANKOSH1	1874	1491	218	933	0.796	13.7	3176
SANKOSH2	5577	2908	63	297	0.521	0.0	76
RAIDAK	2105	1638	128	584	0.778	3.9	3242
DUDKUMAR1	1173	792	59	382	0.675	14.2	3827
DUDKUMAR2	3897	2336	117	685	0.599	0.0	585
DUDKUMAR3	5236	2901	123	590	0.554	0.0	176
DUDKUMAR4	4957	2670	54	222	0.539	0.0	34
TEESTA1	2636	2351	345	1517	0.892	8.5	2943
TEESTA2	3674	2205	59	355	0.600	0.0	340
TEESTA3	4141	2005	74	288	0.492	0.0	39
TEESTA4	3559	1730	140	616	0.486	0.0	48
MANAS1	1258	832	408	1802	0.661	7.7	3657
MANAS2	4074	2101	40	169	0.516	0.0	180

DIBANG	3574	2865	838	1987	0.802	0.1	3019
LOHIT	2319	1886	970	2117	0.813	1.0	3765
SUBANSIRI1	2391	1873	1057	3645	0.783	0.3	3113
SUBANSIRI2	4219	1689	297	1137	0.400	0.0	664
DHARALA	5056	2522	93	397	0.499	0.1	46

5.2 One-dimensional hydrodynamic model

The river flow in MIKE 11 is modelled using a 1D dynamic wave routing based on the Saint Venant equations for unsteady flow MIKE by DHI, 2009. For details on the 1d hydrodynamic modeling approach please refer to LOTUS D6.4.

In the following, we will focus on the Brahmaputra portion of the model only. This part of the model was calibrated to the discharge at Bahadurabad by adjusting the Manning number. A spatially uniform Manning number was calibrated in the hydrodynamic model. The main calibration objective was to calibrate the model's discharge at the station Bahadurabad in Bangladesh, close to the confluence of the Brahmaputra River with the Ganges. The results for the calibration period 2002 to 2007 can be seen in Figure 7. A good fit with a NSE of 0.91, a RMSE of 4955 m^3/s and a mean bias of -7.5% could be obtained.

The validation/data assimilation period includes the years 2010 to 2013, as it starts with the availability of CryoSat-2 data. During that period, in-situ discharge data could only be obtained for the high-flow season (April to October). The model validation result for this period can be seen in Figure 8.

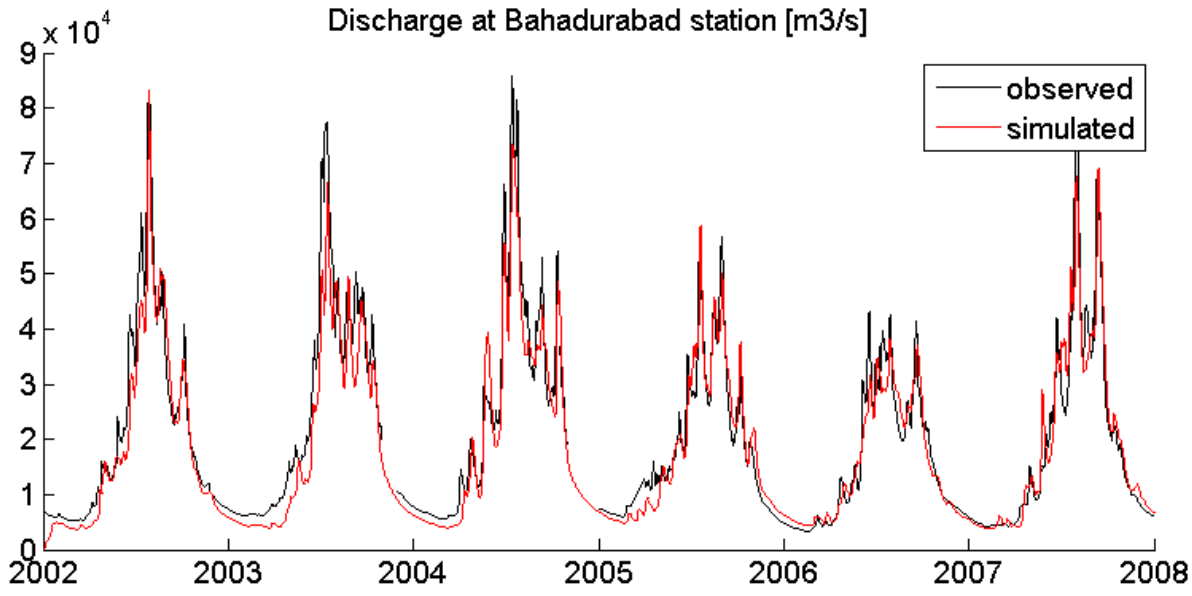

Figure 7: Observed vs. simulated discharge for the Brahmaputra at Bahadurabad station for the calibration period 2002 - 2007

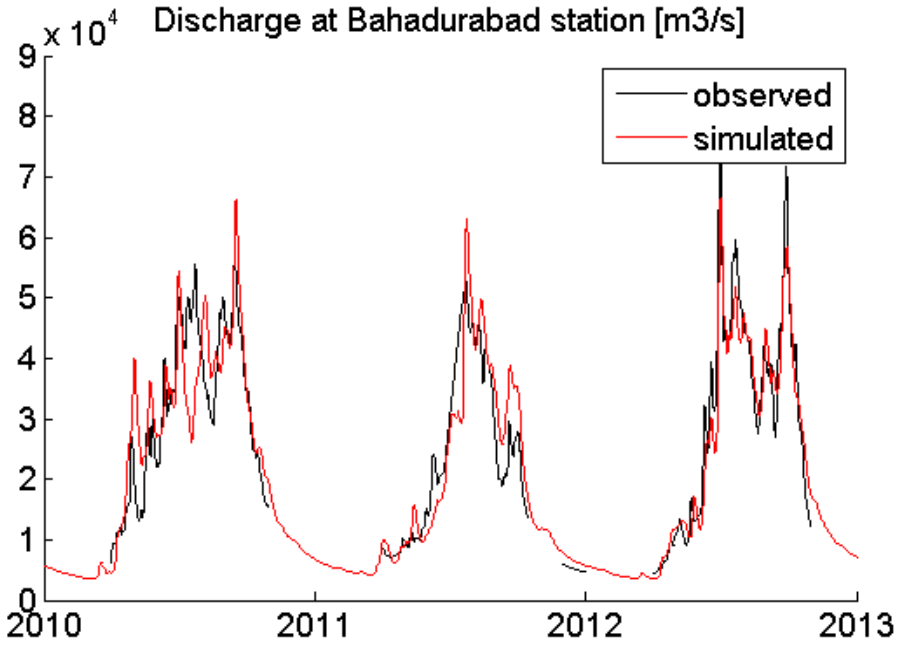

Figure 8: Observed vs. simulated discharge for the Brahmaputra at Bahadurabad station for the data assimilation period 2010 – 2013. Note that observed data only exists for the high-flow periods.

A summary of the results for both periods is presented in Table 5, showing minor decreases in the fit of the model's simulated discharge for the data assimilation period.

Table 5: Number of observations and performance indicators for the station Bahadurabad for the full calibration period 2002 - 2007, the high-flow seasons of 2002 - 2007 and the high flow seasons of 2010 - 2013

	Number of observations	RMSE [m^3/s]	Relative Bias (Q_{sim} - Q_{obs})/ Q_{obs} [-]	NSE [-]
2002 – 2007	5914	4955	-0.075	0.91
2002 – 2007 Apr – Oct only	3792	5471	-0.109	0.90
2010 – 2013 Apr – Oct only	5156	6744	0.048	0.81

The results of the hydrologic-hydrodynamic model for the calibration period 2002 to 2007 with a Nash–Sutcliffe coefficient of 0.91 are good, given the size of the model and the availability of forcing data, using freely available remote sensing only. For the data assimilation period 2010 to 2013 discharge observations at Bahadurabad are only available for the high-flow season. Comparing the model's performance in the two periods therefore has to be done based on data from April to October. The performance of the model in the calibration period stays almost the same – the NSE is only reduced to 0.90. In the validation/data assimilation period the NSE is decreased to 0.81, which is still a very good performance. To some extent, the reduced performance in the validation period could be due issues in the precipitation forcing or changes in the climatic conditions between those two periods.

5.3 Calibration of cross section parameters

No in-situ cross section data was available for model construction. The SRTM DEM was used to derive the rivers' course and a first guess of the cross section datums, using automatic DEM hydro-processing routines. However this can only be seen as a first guess, as the SRTM DEM has a horizontal resolution of 90 meters, and the vertical standard error is in the range of a few meters (Rodríguez et al., 2006). Furthermore the SRTM data cannot represent river bathymetry. A different approach was chosen to ensure that the model accurately reproduces water levels along the river. Cross sections with a simple triangular shape were placed ca. every 50 km along the entire Brahmaputra River (more densely spaced in regions with abrupt changes in bed slope) and then calibrated using the elevations extracted from the SRTM DEM and some rough estimates about bathymetry as a starting point for the calibration.

The cross section calibration was performed after the discharge calibration presented in the previous section. The calibration was based on a combination of data from the Envisat mission and the CryoSat-2 data: The Envisat mission with its 35-day repeat orbit provides virtual station time series. These show water level time series with a 35-day timestep at distinct points in the Brahmaputra River. 13 Envisat virtual stations along the Brahmaputra in the Assam valley (see Figure 10) covering the years 2002 to 2010 were used. The data originates from the ESA River&Lake project (Berry, 2009). CryoSat-2 observations cannot be used directly to extract water level time series. However, due to the drifting orbit, when several years are taken into account, they show the average longitudinal water level profile along the entire river. Both datasets combined provide the necessary information to fully calibrate the model's water levels.

Figure 9 shows the results of step 1 of the water level calibration. For better visibility, the results are all shown as elevations relative to the reference model's cross section datums instead of absolute elevations. The reference model was run with cross section datums derived from the SRTM DEM. It can be seen that the average simulated water levels from the reference model do not accurately represent the CryoSat-2 observations. After calibrating the cross section datums – which resulted in datum adjustments of up to 4 meters – the simulated average water level follows the CryoSat-2 observations more closely. The calibration reduced the RMSE between average simulated water levels and CryoSat-2 observations from 3.04 metres for the reference model to 2.38 meters. The remaining deviation can mainly be explained by seasonal water level variations.

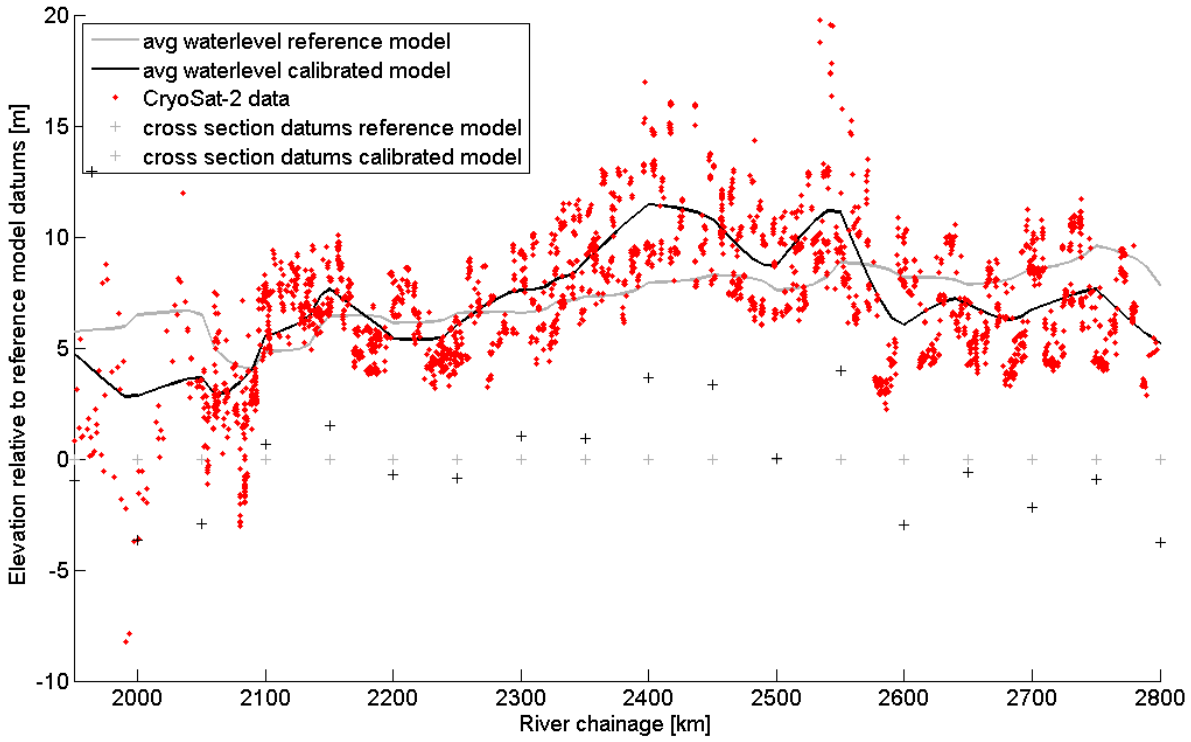

Figure 9: Result of water level calibration step 1 for the Assam valley for the period 2010 to 2013. All levels are shown as elevations relative to the reference model's cross section datums based on the SRTM DEM.

The results of the second step of the cross section calibration - adjusting the cross section angles to fit the simulated water level amplitudes to the Envisat observations - can be seen in Figure 11 for one of the 13 virtual stations. During the calibration, no absolute water levels were used, but time differences. Consequently, Figure 11 shows water levels relative to the time series value at the time of the first Envisat observation.

The change of the cross section shapes to calibrate for water level amplitudes showed to have a relevant effect on the absolute water levels. Subsequently, step 1 of the cross section calibration had to be repeated with the results from step 2.

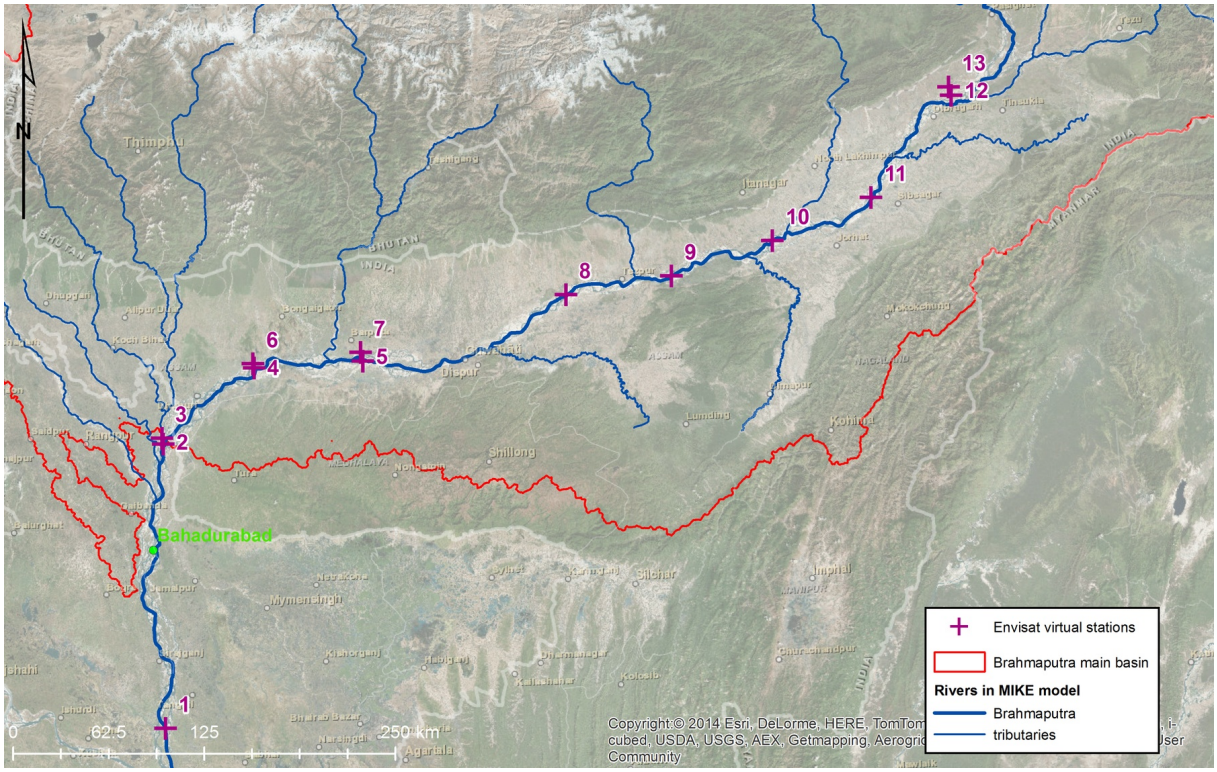

Figure 10: Envisat VS used in step 2 of the cross section calibration. Numbering of VS is the same as in Table 6.

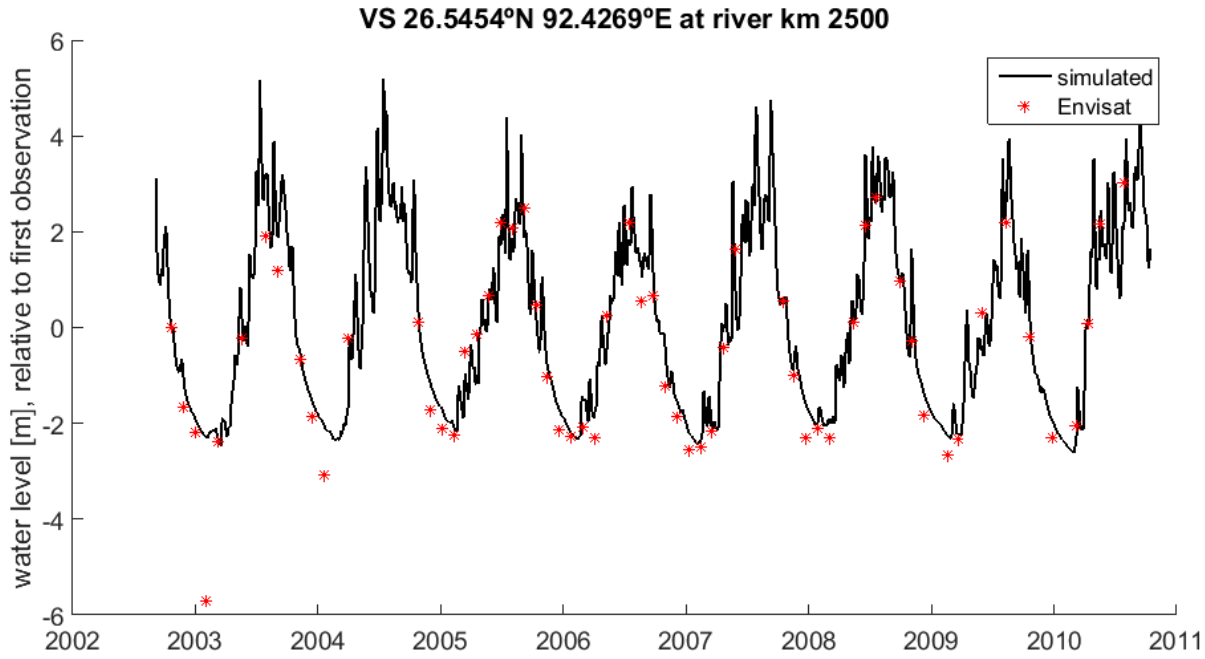

Figure 11: Water levels after step 2 of the cross section calibration for one virtual station (No. 8 in Figure 10 and Table 6). All levels relative to the water levels at the time of the first Envisat observation.

The changes to the cross section were found to have a negligible effect on the discharge routing; hence no discharge recalibration of the model was performed after the water level calibration finished.

The presented cross section calibration offers a way to calibrate water levels in the entire model space without precise knowledge of topography and bathymetry. Synthetic cross sections allow the use of practically any shape, however for the sake of reducing the number of decision variables a simple triangular shape has been chosen. The fitting process is computationally expensive; step 2 takes approximately 1 week on a 20 core calculation server.

Table 6 gives an overview of the results of the cross section calibration.

Table 6: Overview of the results of the cross section calibration

	RMSE (m) pre calibration	ME (m) pre calibration	RMSE (m) post calibration	ME (m) post calibration
Mean water level profile	3.044	-0.136	2.304	0.115
Virtual station 1	2.071	0.047	0.901	0.023
Virtual station 2	1.573	-0.006	0.763	-0.016
Virtual station 3	1.696	-0.010	0.772	-0.020
Virtual station 4	1.770	-0.013	1.046	-0.016
Virtual station 5	2.577	-0.015	2.070	-0.012
Virtual station 6	1.769	-0.025	1.158	-0.012
Virtual station 7	2.433	0.022	2.051	0.040
Virtual station 8	1.650	-0.056	0.947	-0.016
Virtual station 9	2.641	-0.051	2.381	-0.017
Virtual station 10	1.482	-0.033	1.043	-0.007
Virtual station 11	1.533	-0.035	0.757	0.009
Virtual station 12	1.189	-0.039	0.538	-0.002
Virtual station 13	1.070	-0.029	0.533	-0.000

6 Operational modeling and data assimilation for the Brahmaputra

After the water level calibration described in the previous section, CryoSat-2 data from the Assam Valley were assimilated to the hydrodynamic model. The assimilation framework and software architecture is described in LOTUS D6.4. Here, we show the results of a number of data assimilation experiments, using the hydrologic-hydrodynamic model of the Brahmaputra and the Brahmaputra CryoSat-2 dataset.

6.1 Open-loop run

The open-loop run is a probabilistic model run without data assimilation. Model uncertainty is parameterized and an ensemble of model runs is created; the ensemble provides an estimate of the full probability density function (pdf) of all model states and outputs. The performance of the open-loop run is assessed in terms of its sharpness and reliability. Sharpness is a measure of the width of model output pdfs. Reliability requires that actual observations are bracketed by model uncertainty. Sharpness and reliability of a probabilistic model are sometimes combined into one single indicator, the continuous ranked probability score (CRPS). The higher the sharpness and reliability of a probabilistic model, the lower its CRPS. Suitable benchmarks for the performance of probabilistic models are climatology and persistence. Climatology predicts the river discharge for every day of the year as the average of the historical observations for that same day of the year. Persistence predicts the river discharge as the latest available observation prior to the day of interest. A 5-day persistence prediction, for instance, uses today's river discharge as a prediction for the discharge in 5 days from now. For details and definitions of the various indicators and benchmarks please see e.g. Bauer-Gottwein et al., 2015.

In the open-loop run and all DA experiments, it was assumend that the main source of model error is the runoff generated in the NAM subcatchments. This is mainly because of the large uncertainty of the remote sensing precipitation product. Hence, the ensemble was generated by perturbing the catchments' runoffs. Due to the size of the model and the number of subcatchments, the perturbations of the individual catchments have to be correlated in space and time. Otherwise the perturbations of the individual catchments cancel each other out when aggregated in the full model.

Relative runoff error in subcatchment i and time step t (w_t^i) was parameterized as

$$w_t^i = \delta w_{t-1}^i + \varepsilon_t^i$$

where

w_t^i	Relative runoff error in catchment i at time step t
δ	AR1 parameter
ε_t^i	white Gaussian noise

The standard deviation of the random noise contribution ε was assumed constant in time and equal to 0.3. The spatial correlation between noise terms in different catchments was assumed to be the same as the spatial correlation of catchment runoff. The AR1 parameter was set to a value of 0.94 for daily time steps in the open loop run. Ensemble size in the open loop run was 20. Figure 12 and Figure 13 show simulated discharge at Bahadurabad for the individual ensemble members and the ensemble mean. Table 8 provides quantitative performance statistics for the open loop run. The table also provides statistics for climatology and persistence benchmarks. In terms of CRPS, the open loop run outperforms climatology and persistence forecasts beyond a forecasting horizon of 5 days.

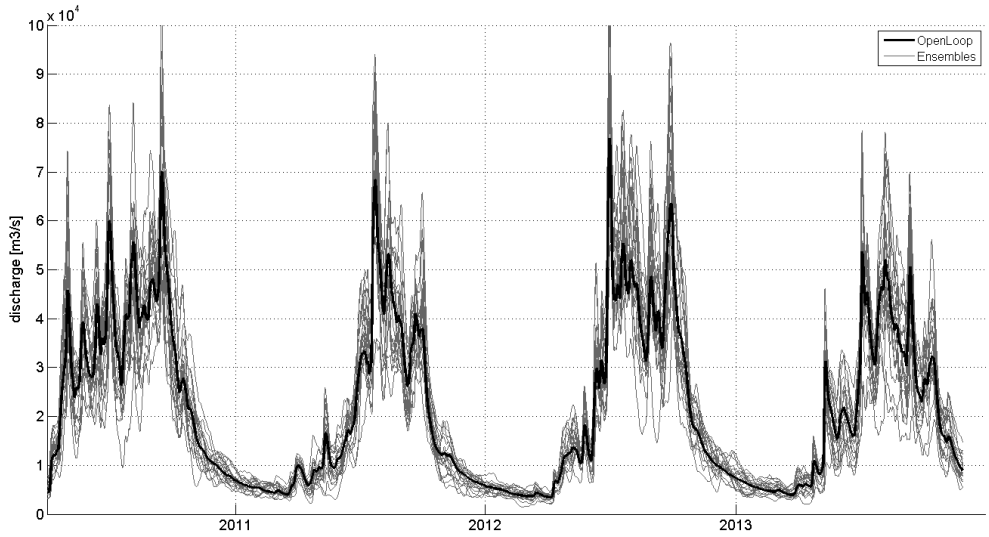

Figure 12: Simulated discharge for the station Bahadurabad in the open-loop run: Individual ensemble members in gray and central prediction in black.

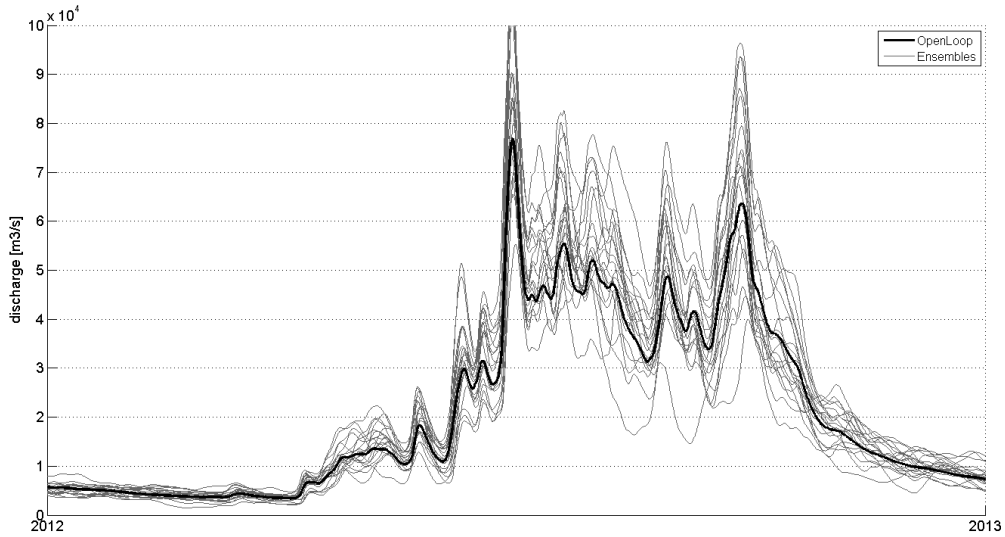

Figure 13: Open-loop run: Zoom-in for the year 2012

6.2 Data assimilation experiments

Three data assimilation experiments were performed, which differ in terms of model error parameterization, assumed observation error, ensemble size, type of data assimilated and localization. Table 7 provides an overview of the specifications for all DA experiments. All DA experiments used the ensemble transform Kalman filter (ETKF) algorithm and in all experiments the spatial correlation of the Gaussian runoff noise term was assumed to be equal to the spatial correlation of runoff. DA experiment 1 uses synthetic observations, created at the exact same locations and times as in the real CryoSat dataset.

DA experiments 2 and 3 use the real Brahmaputra CryoSat dataset. Figure 14 to Figure 19 provide graphical summaries of the results for the three DA experiments, while quantitative performance indicators are listed in Table 8.

Table 7: Specifications for the three DA experiments

	Ensemble size	Filter	Data assimilated	ε	δ	Observation error (m)	localization
DA experiment 1	50	ETKF	Synthetic data	0.25	0.99	0.5	50 km up- and downstream
DA experiment 2	20	ETKF	Real data	0.25	0.94	1	no
DA experiment 3	20	ETKF	Real data	0.25	0.94	0.75	100 km up- and downstream

The outputs show that assimilation of CryoSat data only results in marginal improvements in model performance. One of the most important reasons may be the assumption of uniform observation error for all CryoSat water height data. The observation error is expected to be non-uniform in space and time due to various corrections applied in the processing of water heights (atmospheric correction, geoid, roll bias). It is clear that many possible modifications and enhancements of the DA set-up remain to be tested, as discussed in the next section.

Table 8: Performance overview of benchmarks and various data assimilation runs

Run	NSE (-)	RMSE (m^3/s)	ME (m^3/s)	Coverage of the nominal 95% CI	Sharpness (m^3/s)	CRPS (m^3/s)	Mean of observations (m^3/s)	Number of simulated observations
Climatology	0.6817	8945	-3705	0.9485	22711	4601	24228	1067
Persistence (1-day)	0.9879	1741	69			1046	24228	1067
Persistence (2-days)	0.9573	3265	133			1988	24228	1067
Persistence (3-days)	0.9164	4560	196			2813	24228	1067
Persistence (4-days)	0.8715	5641	258			3536	24228	1067
Persistence (5-days)	0.8266	6534	320			4149	24228	1067
Persistence (6-days)	0.7841	7271	382			4682	24228	1067
Persistence (7-days)	0.7448	7884	445			5161	24228	1067
Persistence (8-days)	0.7079	8416	516			5621	24228	1067
Persistence (9-days)	0.6721	8901	590			6055	24228	1067
Persistence (10-days)	0.6354	9369	667			6445	24228	1067
Open loop	0.7845	7131	3005	0.9292	19167	3995	24228	1067

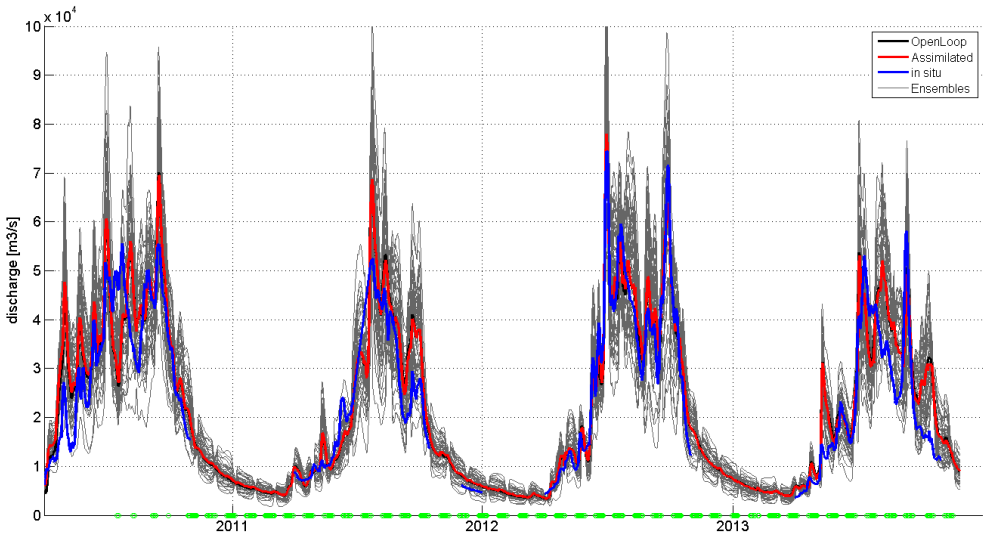

Figure 14: DA experiment 1, discharge at Bahadurabad: Ensemble members in gray, open-loop run in black, assimilated run in red and in-situ data in blue. Green dots indicate timing of CryoSat observations.

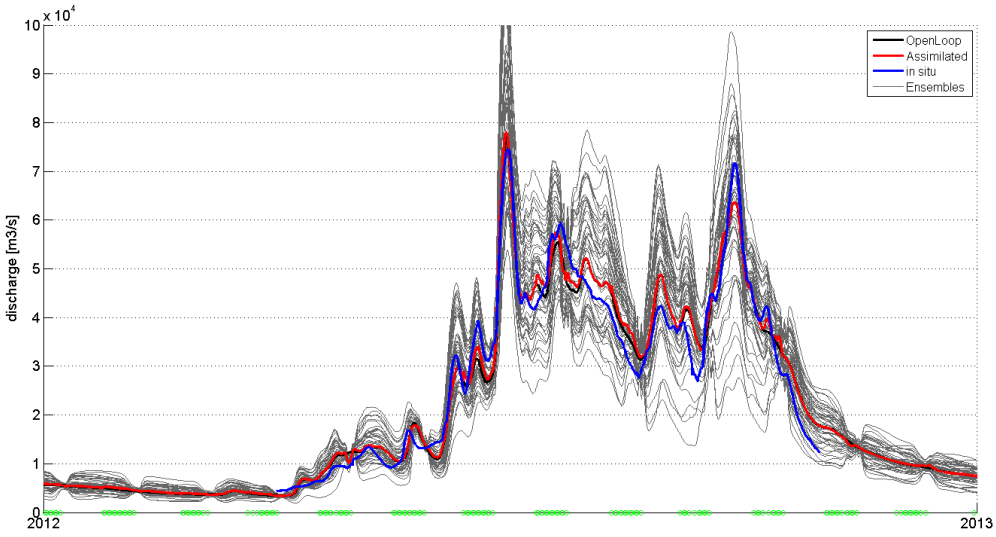

Figure 15: DA experiment 1: Zoom-in for the year 2012

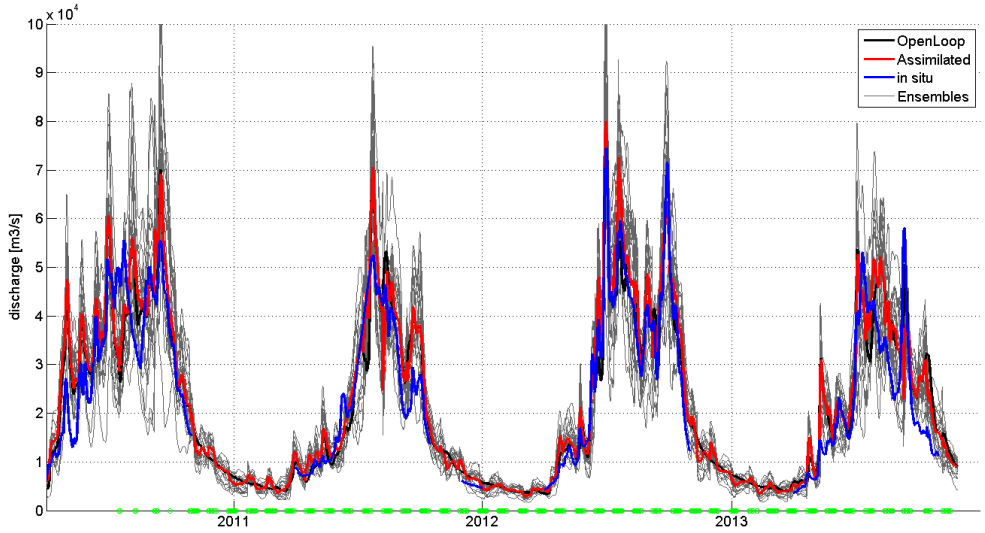

Figure 16: DA experiment 2, discharge at Bahadurabad: Ensemble members in gray, open-loop run in black, assimilated run in red and in-situ data in blue. Green dots indicate timing of CryoSat observations.

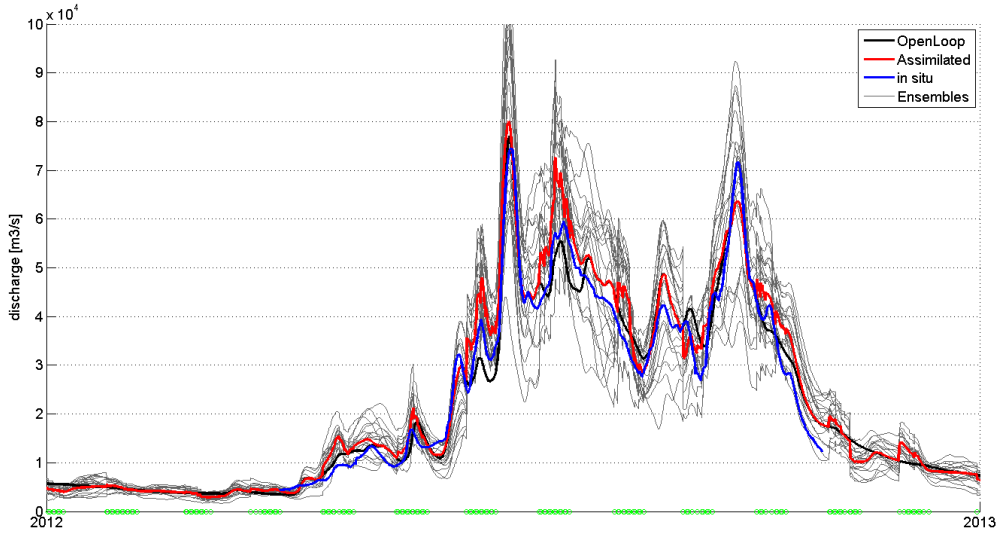

Figure 17: DA experiment 2: Zoom-in for the year 2012

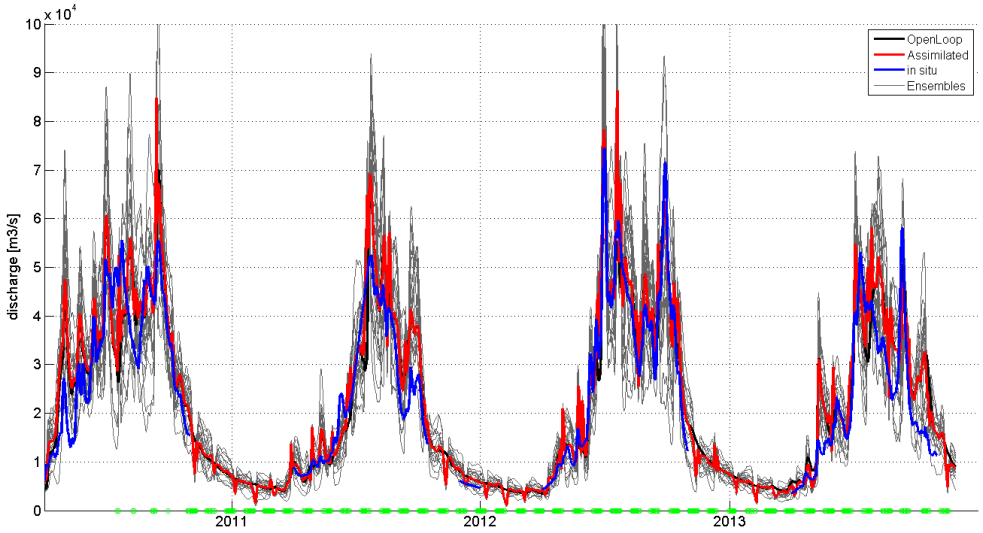

Figure 18: DA experiment 3, discharge at Bahadurabad: Ensemble members in gray, open-loop run in black, assimilated run in red and in-situ data in blue. Green dots indicate timing of CryoSat observations.

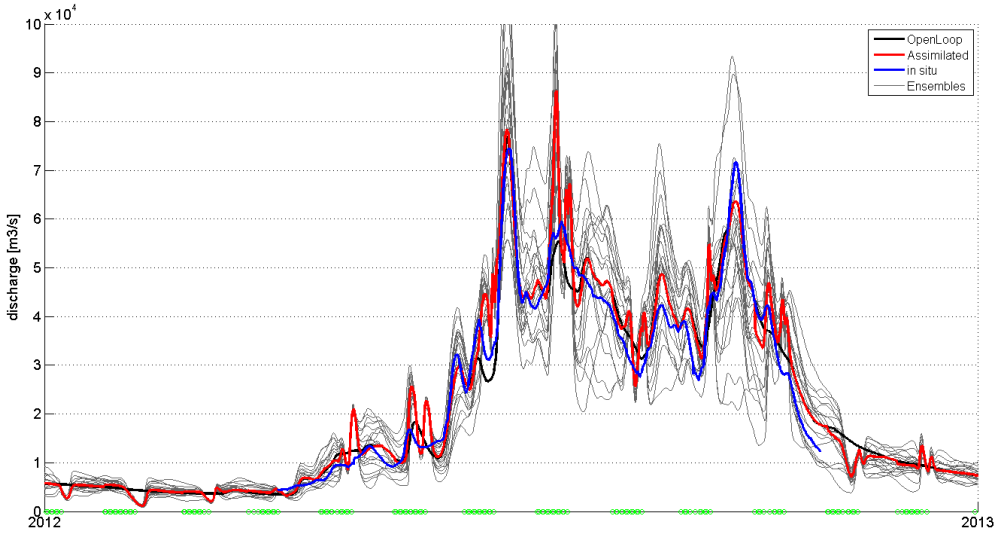

Figure 19: DA experiment 3: Zoom-in for the year 2012

7 Outlook

The field of satellite radar altimetry for inland water monitoring is bound to grow in the near to medium-term future. Several missions are ongoing or scheduled for the near future (Sentinel-3, Jason-3, Jason-CS, AltiKa, HY-2, SWOT). Assimilation of such data to inland water models remains an important research challenge and holds promise for the continued improvement of operational hydrologic forecasting.

The focus of this study was to develop the technical knowledge base and algorithms to be able to assimilate CryoSat radar altimetry data to large-scale hydrologic-hydrodynamic models. While this objective was achieved, performance improvement of hydrologic forecasts remained marginal for the data assimilation experiments reported in this study. There are a number of aspects that should be further investigated with the presented modeling and DA setup, including:

- Effect of buffer zone around the permanent water mask. This will make sure that only echoes placed centrally over open water surfaces will be assimilated to the hydrodynamic model. Height estimates derived from such echoes are expected to be of higher accuracy.
- Instead of working with a uniform observation uncertainty, the observation uncertainty can be calculated as the standard deviation of height estimates pertaining to the same cluster of measurements. Measurements with a lower uncertainty will then get a larger weight in the assimilation scheme than highly uncertain measurements.
- Spatial subsetting. While the cross section calibration reported in this study ensured a global fit between simulated river heights and the CryoSat dataset, there will be bias between model and observations locally. It should be investigated if erroneous or overshooting updates in the assimilation scheme are consistently produced by measurements over distinct stretches of the river.
- Extending the assimilation period to include 2014 and 2015.

8 Conclusions

This study has established the technical basis for the assimilation of CryoSat radar altimetry data to hydrologic-hydrodynamic models. The approach was demonstrated practically for the Brahmaputra basin. The approach is scalable and can be extended to other basins and to continental/global coverage. The results we have so far do not show clear performance improvements of operational hydrological models that are attributable to the CryoSat river height dataset. The CryoSat dataset and inland water altimetry in general may become a key data source for water managers in the region due to its impartial nature, open accessibility to all low cost. The impact of the dataset will increase with enhanced spatio-temporal resolution available from the combination of multiple missions and with a better understanding of the error statistics of the altimetry data.

References

APHRODITE's Water Resources, 2014. APHRODITE's Water Resources - Home [WWW Document].

Bauer-Gottwein, P., Jensen, I.H., Guzinski, R., Bredtoft, G.K.T., Hansen, S., Michailovsky, C.I., 2015. Operational river discharge forecasting in poorly gauged basins: the Kavango River basin case study. Hydrol. Earth Syst. Sci. 19, 1469–1485. doi:10.5194/hess-19-1469-2015

Becker, M., da Silva, J., Calmant, S., Robinet, V., Linguet, L., Seyler, F., 2014. Water Level Fluctuations in the Congo Basin Derived from ENVISAT Satellite Altimetry. Remote Sens. 6, 9340–9358. doi:10.3390/rs6109340

Berry, P., 2009. River and Lake Product Handbook v3.5.

Biancamaria, S., Durand, M., Andreadis, K.M., Bates, P.D., Boone, a., Mognard, N.M., Rodríguez, E., Alsdorf, D.E., Lettenmaier, D.P., Clark, E. a., 2011a. Assimilation of virtual wide swath altimetry to improve Arctic river modeling. Remote Sens. Environ. 115, 373–381. doi:10.1016/j.rse.2010.09.008

Biancamaria, S., Hossain, F., Lettenmaier, D.P., 2011b. Forecasting transboundary river water elevations from space. Geophys. Res. Lett. 38, L11401. doi:10.1029/2011GL047290

Birkinshaw, S.J., Moore, P., Kilsby, C.G., O'Donnell, G.M., Hardy, A.J., Berry, P.A.M., 2014. Daily discharge estimation at ungauged river sites using remote sensing. Hydrol. Process. 28, 1043–1054. doi:10.1002/hyp.9647

Central Water Commission, 2009. Integrated Hydrological Data Book (non-classified river basins). New Delhi.

Google, 2015. Google Earth Engine - Landsat 7 32-Day NDVI Composite [WWW Document].

Jarvis, A., Reuter, H.I., Nelson, A., Guevara, E., 2008. Hole-filled SRTM for the globe Version 4, available from the CGIAR-CSI SRTM 90m Database.

Kleinherenbrink, M., Ditmar, P.G., Lindenbergh, R.C., 2014. Retracking Cryosat data in the SARIn mode and robust lake level extraction. Remote Sens. Environ. 152, 38–50. doi:10.1016/j.rse.2014.05.014

Michailovsky, C.I., Milzow, C., Bauer-Gottwein, P., 2013. Assimilation of radar altimetry to a routing model of the Brahmaputra River. Water Resour. Res. 49, 4807–4816. doi:10.1002/wrcr.20345

MIKE by DHI, 2009. MIKE 11 - A Modelling System for Rivers and Channels - Reference Manual.

NASA, 2015. NASA Science Missions - SWOT [WWW Document].

Nielsen, S.A., Hansen, E., 1973. Numerical simulation of the rainfall runoff process on a daily basis. Nord. Hydrol. 4, 171–190.

Rodríguez, E., Morris, C.S., Beiz, E.J., 2006. A Global Assessment of the SRTM Performance. Photogramm. Eng. Remote Sens. 72, 249 – 260.

Song, C., Ye, Q., Cheng, X., 2015. Shifts in water-level variation of Namco in the central Tibetan Plateau from ICESat and CryoSat-2 altimetry and station observations. Sci. Bull. 60, 1287–1297. doi:10.1007/s11434-015-0826-8

Tarpanelli, A., Brocca, L., Barbetta, S., Faruolo, M., Lacava, T., Moramarco, T., 2014. Coupling MODIS and Radar Altimetry Data for Discharge Estimation in Poorly Gauged River Basins. IEEE J. Sel. Top. Appl. Earth Obs. Remote Sens. 8, 1–8. doi:10.1109/JSTARS.2014.2320582

Tropical Rainfall Measurement Mission Project (TRMM), 2011. TRMM 3-Hourly 0.25 deg. TRMM and Others Rainfall Estimate Data.

Villadsen, H., Andersen, O.B., Stenseng, L., Nielsen, K., Knudsen, P., 2015. CryoSat-2 altimetry for river level monitoring - Evaluation in the Ganges-Brahmaputra basin. Remote Sens. Environ. 168, 80–89.

Yamazaki, D., Lee, H., Alsdorf, D.E., Dutra, E., Kim, H., Kanae, S., Oki, T., 2012. Analysis of the water level dynamics simulated by a global river model: A case study in the Amazon River. Water Resour. Res. 48, n/a–n/a. doi:10.1029/2012WR011869

Yoon, Y., Durand, M., Merry, C.J., Clark, E. a., Andreadis, K.M., Alsdorf, D.E., 2012. Estimating river bathymetry from data assimilation of synthetic SWOT measurements. J. Hydrol. 464-465, 363–375. doi:10.1016/j.jhydrol.2012.07.028